-RESEARCH PAPER-

International Journal of Mining and Geo-Engineering

IJMGE

IJMGE 58-2 (2024) 211-220

DOI: 10.22059/IJMGE.2024.367398.595116

Blasted muckpile modelling in open pit mines using an artificial neural network designed by a genetic algorithm

S. M. Mahdi Mirabedi [a], Mehdi Rahmanpour [a, *], Yousef Azimi [b] and Hassan Bakhshandeh Amnieh [a]

[a] *School of Mining, College of Engineering University of Tehran, Tehran, Iran.*

[b] *Research Centre for Environment and Sustainable Development, RCESD, Department of Environment, Tehran, Iran.*

Article History:

Received: 09 December 2023.

Revised: 01 January 2024.

Accepted: 09 January 2024.

ABSTRACT

The shape of a blasted rock mass, or simply muckpile, affects the efficiency of loading machines. A muckpile is defined with two main parameters known as throw and drop, while several blasting parameters will influence the muckpile shape. This paper studies the prediction of the muckpile shape in open-pit mines by applying an artificial neural network designed by a genetic algorithm. In that regard, a genetic algorithm has been used in preparing the neural network architecture and parameters. Moreover, input variables have been reduced using the principal component analysis. Finally, the best models for predicting throw and drop determined. Analyzing the performance of the proposed models indicates their superiority in predicting the muckpile shape. As a result, the Mean Squared Error of the throw was 0.53 for the training data and 1.24 for the testing data. While for the drop, the errors were 0.45 and 0.58 for the training and testing data, respectively. Furthermore, the sensitivity analysis shows that specific-charge effects drop and throw more.

Keywords: *Hybrid genetic algorithm neural network, Blasting, Muckpile, Principal component analysis.*

1. Introduction

Rock blasting remains the most efficient method for loosening and fragmenting rocks in mining operations, constituting about 15–20% of the total mining cost [1-3]. The blasting operation starts with rock mass fracturing by the shock waves from the detonating explosive. Then expanding of explosive gases will develop cracks and fractures within the rock mass. The blasting energy will heave and move the fragmented rock mass to form a muck pile. The diggability of a muckpile is related to the specifications of fragmented rock mass and its movement. The Muckpile Shape (MSh) and particle size distribution have essential effects on productivity, performance, and the cost of downstream mining activities, such as loading, hauling, and crushing [4-12]. The objective of blasting in a mine should be to generate a muckpile that can be loaded, transported, and crushed efficiently [13-15]. In surface coal mines, the blasting operation is designed to move the blasted waste rock into the inner dump area. If 34% of the broken rock is cast into the inner dump, about 1/3 stripping cost is saved. If draglines are utilized, it should be noted that for draglines, the MSh is of more interest than the percentage of blasted rock moved into the inner dump [16].

Different MShs can occur after blasting, as shown in Figure 1. In any surface blasting operation, there is always a desired MSh. The suitable MSh is determined based on the features of the blasting blocks and the equipment utilized. Any loading machine can work efficiently in a particular MSh. For example, when shovels are used, a high muck level is desired [17].

Front-end loaders generate a relatively small break-out force and are better utilized in low, flat-lying, and loose muckpiles. Then, the blasts should provide acceptable displacement, enough rock swelling, high fragmentation, and a reduced height for the muckpile (Figure 1.a) in cases where front-end loaders are used. In other words, for front-end loaders, the blasting operation should generate a muckpile that spreads the rocks over the bench. In this case, the blasted area needs excessive clean-ups. However, the operation area is safe, and reaching high productivity with a front-end loader is possible. In brief, the condition in Figure 1.a is ideal for front-end loaders, but for shovels, because of the time required for dozing and clean-up, shovel productivity is reduced.

Shovels generate a significant break-out force, filling the bucket when moving in the vertical direction. Therefore, the efficiency of shovels depends on the muckpile height. For such machines, the blasting operation should provide adequate fragmentation accompanied by a muckpile that is not spread. Figure 1.b shows the optimum and safe conditions for shovel operation with minimum clean-up and high productivity [18]. Increasing muckpile height improves shovel efficiency.

Nevertheless, it is noteworthy that a safe operation requires limited muckpile height (Figure 1.c). Generally, the MShs can be characterized by throw and drop (Figure 2). "Throw" describes the spreading of a muckpile, and "drop" implies the vertical lowering of the blasted muckpile concerning the bench height.

The MShs is governed by (1) blast geometry, including bench height, blasthole inclination, burden, spacing, and stemming, (2) powder factor,

* Corresponding author. *E-mail address:* : mrahmanpour@ut.ac.ir (M. Rahmanpour).

and (3) initiation sequence [19]. The blast geometry is a significant aspect of blasting design and has a pronounced effect in practice on rock fragmentation and broken rock movement. For example, suppose the burden is too small to provide suitable confinement to the gas pressure. In that case, gas energy leaks into the atmosphere before contributing to fragmentation or displacement. Besides, the benefits of inclined blasthole are better fragmentation and better removal of the blasted rocks. A uniform burden along the blastholes leads to a better shot direction. Stemming is another critical factor. Insufficient stemming will increase the probability of free gas escaping into the atmosphere. However, excessive stemming leads to many boulders, poor muckpile swelling, and an elevated vibration.

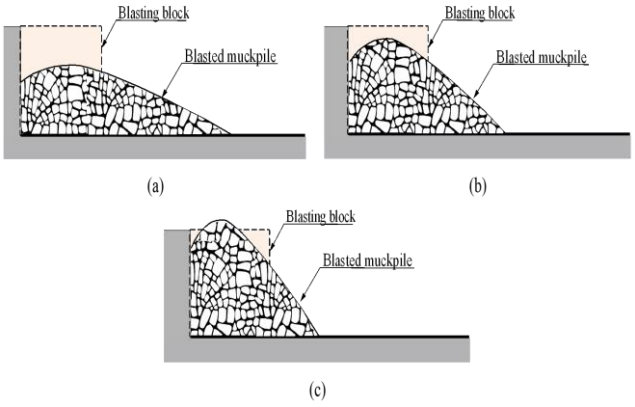

Figure 1. The examples of MShs (Adapted from [17]).

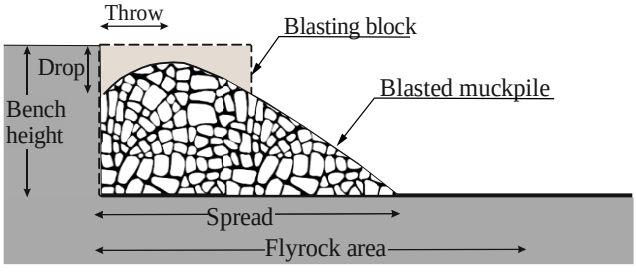

Figure 2. Muckpile shape (Adapted from [16]).

The powder factor or specific charge depends on the rock condition and blast geometry. Studies show that for a given rock condition, an excess powder factor will cause excessive throw and backbreaks [19, 20]. It should be noted that even with the same drilling patterns, different timing and delays will result in different displacements. In practice, the rock displacement is strongly affected by delay time [21]. As the delay between rows decreases, the vertical component of displacement increases while the horizontal component decreases. The short delay increases rock density resulting from wave collision between holes and increases throw. Researchers have tried to model and predict the MSh based on rock conditions and blast parameters, but it is still a challenging issue [22]. Yang et al. [23] and Yang and Kavetsky [24] presented an approach to model the muckpile formation process. Their model calculates diggability contours and provides several muckpile cross-sections. The model needs to be calibrated to the site condition. Morin and Ficarazzo [25] presented a simulation-based approach, Singh et al. [26] conducted experiments to optimize the throw distance in cast blasting, Mencacci et al. [27] applied the six-sigma methodology, and Muller et al. [28] introduced an approach to evaluate and control the fragmentation and MSh. They measured grain size and muckpile slope as the factors governing the MSh. Rosa and Thornton [29] discussed various technologies used to measure blasted rock movements and the difficulties in modelling these movements. Choudhary [30] and Choudhary and Rai [31] conducted field studies to evaluate the effects of blasting patterns and stemming plugs on the fragmentation and MSh. Cardu et al. [32] assessed the impact of blasting sequence on rock fragmentation and muckpile. They defined the MSh as the ratio of the muckpile spread length normalized to the blasthole height.

The regression analysis is quite appealing for predicting the MSh, but the results are poor concerning the degree of non-linearity [33-36]. Moreover, several inter-related controllable (blast-geometry and explosive) and uncontrollable (geological and geomechanical) parameters exist. Many soft computing techniques have been applied to predict the MSh. Some researchers used Artificial Neural Networks (ANNs) to determine the parameters affecting the MSh [37-39]. They noticed that charge density, rock density, and burden are the most influential parameters on the MSh. Vasylchuk and Deutsch [40] consider the effect of muckpile displacement on grade control in open-pit mines. Others conducted fieldworks and studied the effects of blasting parameters, explosive properties, and fragmentation size on the MSh [41, 42]. They noticed that burden, bench height, heave energy, and fragmentation size strongly influence the MSh. More recently, hybrid models have been of more interest [43-49]. Hybrid models integrate an optimization model with a prediction model to enhance the prediction performance.

The performance of an ANN depends on its architecture and training process. Moreover, the ANN architecture is case-specific and should be established based on the problem. Typically, the architecture is determined via a trial-and-error approach, which does not guarantee the optimum architecture. Researchers have proposed neuro-evolutive algorithms to mitigate the shortcomings of the trial-and-error approach [50-52]. This paper aims to enhance the ANN performance and the MSh prediction accuracy using a Genetic Algorithm (GA). The GA will determine the ANN architecture, including training algorithms, transfer functions, number of neurons and layers, and the maximal epochs. The proposed algorithm will mitigate the shortcomings of the trial-and-error approach. Moreover, this study analyzes the effect of using the Principal Component Analysis (PCA) method to preprocess the parameters. The PCA is applied to reduce the complexity of input parameters for the ANN. Finally, a novel hybrid of GA, PCA, and ANN is successfully developed to predict the MSh parameters.

2. Methodology

2.1. Hybrid Genetic Algorithm - Artificial Neural Network

ANNs are biologically inspired learning systems that emulate the computational powers of the human brain. The learning process adopts the weight of interlinked neurons. The numerical weight associated with each link expresses the strength or importance of each neuron. Thus, iterative and adaptive weight modification enables the system to learn the particular aspects of the problem [53, 54].

The Multilayer Perceptron Model (MLP) is a widely accepted ANN model. A perceptron calculates the output signal by employing a linear combination of available inputs. Then, an activation function changes the output signal to get the output y. The structure of MLPs includes an input layer, an Output Layer (OL), and at least one Hidden Layer (HL) (Figure 3).

When the MLP structure is determined, the training process starts. The calculation process consists of two steps. In the first step, the inputs are processed in the HL(s), and the results are passed to the OL. In the second step, the expected outputs are calculated. When the expected outputs are calculated, one can determine the prediction errors. The system aims to minimize prediction errors. Despite the advantages of ANNs, designing the ANN structure is a complex task. The GA is valuable for finding approximate solutions to complex non-linear problems. The GA is a search-based algorithm that initiates with a randomly generated population and evolves toward a better population. In the GA, the individuals are selected by elitism. In each population, individual solutions are ranked based on a predefined fitness function. Elites or highly valued individuals have the chance of being selected as the parents of the next generation. In the crossover process, features or chromosomes of parent individuals are exchanged to produce new individuals called offspring. In the mutation process, the process of

changing genes inside a chromosome is carried out. This process is repeated until a predetermined termination criterion is met. Finally, the best offspring is returned to represent the optimum solution [55-56]. Before applying the GA for the ANN improvement, one must define the objective function and encoding system.

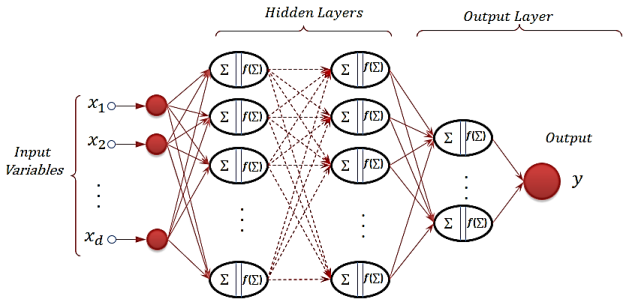

Figure 3. The MLP structure.

Objective function

The purpose of using GA is to enhance the ANN performance by optimizing its architecture. Hence, the objective function is defined as (Eq. 1).

$$f_{obj} = \underbrace{a e^{f(s)}}_{F_1} \times \underbrace{1 + \varphi.x + \omega.y}_{F_2} \times \underbrace{a_1 \times e + b}_{F_3} \times \underbrace{\left(\frac{1}{n}\sum_{i=1}^{n}\left|\frac{(Y_i - T_i)}{Y_i}\right| + \frac{1}{m}\sum_{i=1}^{m}\left|\frac{(Y_i - T_i)}{Y_i}\right|\right)}_{F_4} \quad (1)$$

where, f_{obj} is the objective function, a is a constant, and $f(s)$ is a function of bias (s). In this work, $a=1$ and $f(s)= 0.01 \times s$. x is the number of test records having a relative error of 15 to 25, and y is the number of test records whose relative error is more than 25. φ *and* ω represent the importance levels of x and y. In this work, $\varphi = 0.33$ and $\omega = 1$ are considered. a_1 and b are constants and e represent the training epochs. In this work, $a_1 = 2 \times 10^{-5}$ and $b = 1$. T_i and Y_i are the estimated and the actual outputs, respectively. n is the number of training data, and m is the number of testing data.

In Eq. 1, the term F_1 is the feed-forward architecture criterion, and it prefers small architectures. Small architectures avoid over-fitting, augments the generalization ability of the ANN and accelerate the training process. The term F_2 is the solution space consistency, and it computes the prediction error of testing data. The term F_3 represents the learning time criterion. The Term F_4 is the average errors in training and generalization. It represents the memorization ability of ANNs, and estimates how well the network is trained, quantitatively. Moreover, it computes the power of the ANN to respond to new samples.

Encoding the optimization model

The GA embedded in Matlab® is employed for optimizing the objective function (Eq. 1). The decision vector (X) must contain the number of HLs and the respective number of neurons, activation function, training algorithm, and the maximum number of epochs. In that regard, the chromosome is designed to fulfill the requirements of the decision vector. The decision vector is composed of four distinct sectors. The first sector of the chromosome includes x_1 to x_3 indicating the neurons numbers in three HLs. The second sector contains x_4 to x_7 that define the activation functions between consecutive layers. The third sector is x_8, which describes the training algorithm, and the last sector (i.e., x_9) shows the maximum epochs. Eq. 2 indicates the general form of the problem. The penalty approach is adopted to satisfy integer constraints [57, 58].

$$MinZ = F_1(X) \times F_2(X) \times F_3(X) \times F_4(X) \quad (2)$$

$$s.t: \quad 1 \le x_i \le ubn, \quad \forall i = 1,2,3$$
$$1 \le x_i \le ubtf, \quad \forall i = 4,5,6,7$$
$$1 \le x_8 \le ubtr$$

where, ubn is the maximum number of neurons in HLs,
$ubtf$ controls the type of activation function,
$ubtr$ control the type of training algorithm, and
lb and ub constrain the number of epochs.

Thus, the optimal solution of the model in Eq. 2 corresponds to an ANN architecture with the lowest possible training and generalization errors.

2.2. Principle Component Analysis (PCA)

ANN models require a significant amount of training data, which is rarely feasible in real-world cases. Acquiring representative datasets is constrained by the high cost of large-scale experiments, which is the case in mining engineering. However, when training data is limited, the ANN forecasters are susceptible to over-fitting, which means rigid memorization of training data but cannot predict new data. As a result, ANN models based on small datasets exhibit unstable performance. Therefore, the applications of ANNs on small and imbalanced datasets require careful analysis [59-63]. Furthermore, datasets with many parameters and limited training sets pose challenges for learning algorithms [64]. Several attempts have been made to tackle the learning problem in small datasets [64, 66, and 65]. Variable reduction in the MLP networks seems to increase the network generalization [66].

According to literature, the MSh depends on various correlated parameters. Therefore, it provides an opportunity to reduce the number of input features. Dimensionality reduction is an essential topic in learning algorithms. The selected subset is still representative and retrieves a large proportion of the information from the original dataset. Eventually, in any learning algorithm, the reduced subset can be utilized. Therefore, developing a new model based on a limited dataset is necessary. In that regard, this study analyzes the effect of using the PCA to reduce the complexity of input parameters for the ANN. The PCA generates new Principal Components (PCs) to replace the original parameters. The PCA transforms some correlated variables into linearly uncorrelated new ones (Eq. 3) [67].

$$PC_j = \sum w_{ji} x_i = w_{j1}x_1 + w_{j2}x_2 + \ldots + w_{ji}x_i \quad (3)$$

where, PC_j is the jth principal component,
x_i is the standardized score of the original variable i, and
w_{ji} is the coefficient score of variable i, for the component PC_j.

A PC is a type of variable that could not be measured directly. All PCs are linearly uncorrelated. Therefore, no redundant information exists in the final components. The components are defined such that the variance of the first few PCs covers 80% of the total variance. To be sure that the new components are independent, the dataset must have a normal distribution.

2.3. Multi-criteria system for best model selection

As stated, the MSh is defined by throw and drop. Then, two-hybrid GA-MLP and two PCA-GA-MLP models are developed for the MSh prediction. The performances of these models will be evaluated through four indices (Eq. 4 to 7). The indices include Nash-Sutcliffe Efficiency (NSE), Root Mean Square Error (RMSE), Mean Absolute Error (MAE), and Median Absolute Error (MEDAE). According to the indices, alternate models are sorted in descending order and ranked. This ranking system is done separately for all alternate models for training, testing, and validation datasets. At last, the model with the lowest total score is selected as the best model.

$$NSE = 1 - \frac{\sum_{i=1}^{n}(T_i - Y_i)^2}{\sum_{i=1}^{n}(T_i - mean(T_i))^2} \quad (4)$$

$$RMSE = \sqrt{\frac{1}{n}\sum_{i=1}^{n}(T_i - Y_i)^2} \quad (5)$$

$$MAE = \frac{1}{n}\sum_{i=1}^{n}(T_i - Y_i)^2 \quad (6)$$

$$MEDAE = median|T_i - Y_i| \forall i = 1, \ldots, n \quad (7)$$

3. Implementation and results

In this section, the GA-MLP and PCA-GA-MLP models were applied to the MSh prediction, specified by throw and drop. Various parameters may govern the MSh, including the bench height, burden, spacing, sub-drilling, stemming, charge weight, width to height ratio, drill penetration rate, specific charge, primer consumption, number of benches, number of holes, and firing pattern. The input data are selected from 82 blasting instances in similar ground conditions from [24, 30, 31, 34-37]. The specification of the dataset is summarized in Table 1. Moreover, each experiment conducts a V-cut firing pattern with constant inter-hole blast timing.

3.1. First scenario: GA-MLP

The dataset is partitioned, and 70%, 15%, and 15% of data were used for training, validation, and testing phases, respectively. The GA model setting is given in Table 2. The maximum number of hidden layers is considered three, which is more than adequate for most engineering applications. Chromosomes with lengths of 5, 7, and 9 bits are considered for networks containing 1, 2, and 3 HLs, respectively. The GA population size and maximum generation were considered 100 and 50, respectively. The crossover rate is 0.85, and the mutation rate is 0.01. Moreover, binary tournament selection is chosen for the selection operation.

The GA-MLP was used to perform 30 independent runs with the same training, validation, and testing datasets. According to the results, the optimum MLP network performances are given in Table 3. The optimum networks for throw and drop are illustrated in Figure 4. For the optimum networks, the analysis of measured and estimated values of throw and drop for different vector data is shown in Figure 5.

3.2. Second scenario: PCA-GA-MLP

This section evaluates the effect of variable reduction on the performance of the MLP networks. In that regard, after determining the PCs, they are fed into the PCA-GA-MLP algorithm. The settings used in the PCA-GA-MLP are the same as GA-MLP. The difference in the number of input variables is reduced from 10 to four. Like the first scenario, 30 independent runs with the same data were done, and the best network was chosen. The optimum network is shown in Figure 6. A comparison of measured and estimated values for the training and testing data is shown in Figure 7. The performance of the optimum MLP networks is given in Table 4.

Table 1. The dataset specification.

Data type	Parameters	Min	Max	Ave.	Standard deviation
Input	Bench height (m)	6.00	10.00	6.89	1.41
	Burden (m)	2.80	3.20	2.90	0.13
	Spacing (m)	3.20	4.50	3.73	0.45
	Sub drill length (m)	0.50	1.00	0.64	0.23
	Stemming length (m)	1.50	2.50	1.77	0.32
	Charge weight (ton)	0.37	2.60	1.14	0.58
	Length to width ratio	0.78	12.50	3.94	2.60
	Specific Charge (kg/t)	0.12	0.29	0.19	0.04
	Number of rows	2.00	7.00	4.00	1.43
	Number of holes	13	110	43.10	21.46
	Firing pattern	V cut	-	-	-
Output	Throw	3.85	14.25	9.89	2.82
	Drop	0.00	6.00	2.97	1.17

Table 2. Chromosome encoding setting for the GA.

Gene	Configuration	Lower bound	Upper bound
x_1	number of neurons in hidden layers (NNHL)	1	40
x_2		1	40
x_3		1	40
x_4	Transfer/activation Functions (TRF):	1	11
x_5	(1) 'tansig', (2) 'logsig', (3) 'purelin', (4) 'elliot2sig',	1	11
x_6	(5) 'elliotsig', (6) 'radbas', (7) 'poslin', (8) 'radbasn',	1	11
x_7	(9) 'tribas', (10) 'satlin' and (11) 'satlins'	1	11
x_8	Training Algorithms (TRA): (1) Levenberg-Marquardt (trainlm), (2) Bayesian Regularization (trainbr), (3) Gradient Descent with Momentum (traingdm), (4) BFGS Quasi-Newton (trainbfg), (5) Scaled Conjugate Gradient (trainscg) and (6) Variable Learning Rate Gradient Descent (traingdx)	1	6
x_9	maximum number of epochs (MNEP)	1000	2500

(a)

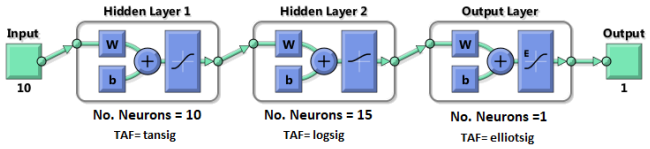

(b)

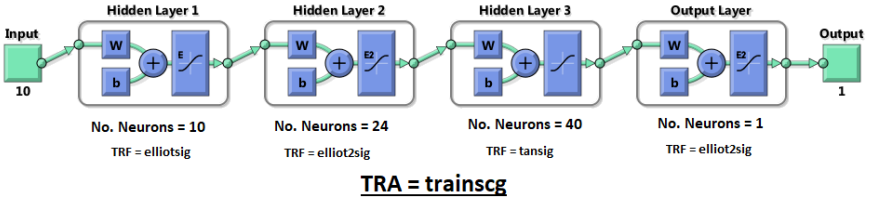

Figure 4. The optimum network architecture (a). Throw (b). Drop.

Table 3. The GA-MLP results for throw and drop.

Output	Data	NSE	RMSE	MAE	MEDAE
Throw	ALL	0.871	0.842	0.571	0.339
	Train	0.946	0.534	0.358	0.212
	Test	0.764	1.247	0.992	0.795
	validation	0.652	1.352	1.138	0.865
Drop	ALL	0.892	0.491	0.371	0.285
	Train	0.913	0.455	0.328	0.253
	Test	0.819	0.584	0.488	0.356
	validation	0.839	0.539	0.443	0.503

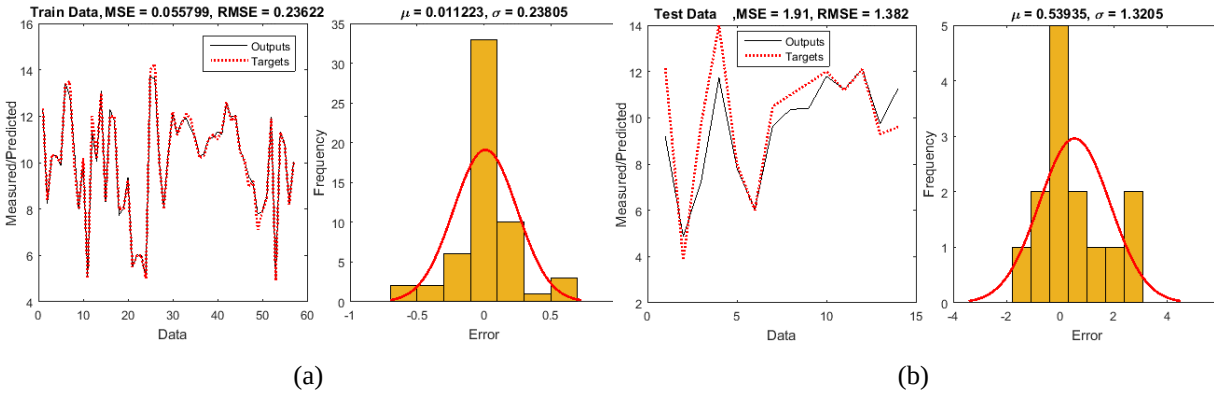

(a) (b)

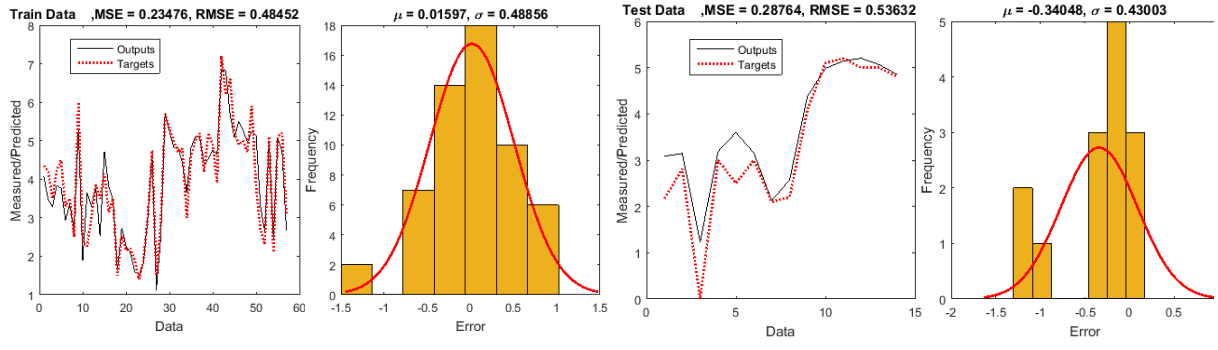

(c) (d)

Figure 5. The measured and estimated values, and estimation error histogram for the optimum MLP. (a) training data of throw, (b) test data of throw (c) training data of drop, (d) test data of drop

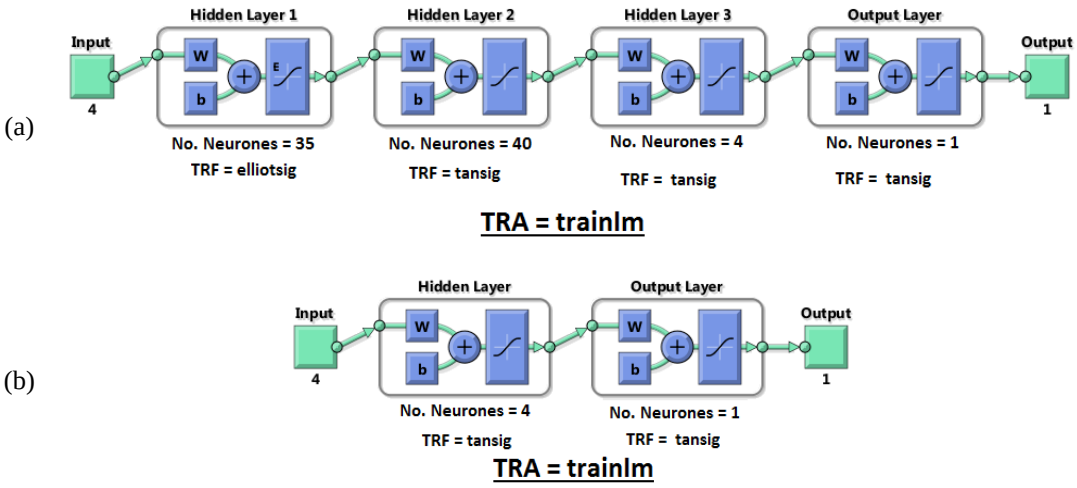

Figure 6. The optimum network architecture (a). Throw (b). Drop.

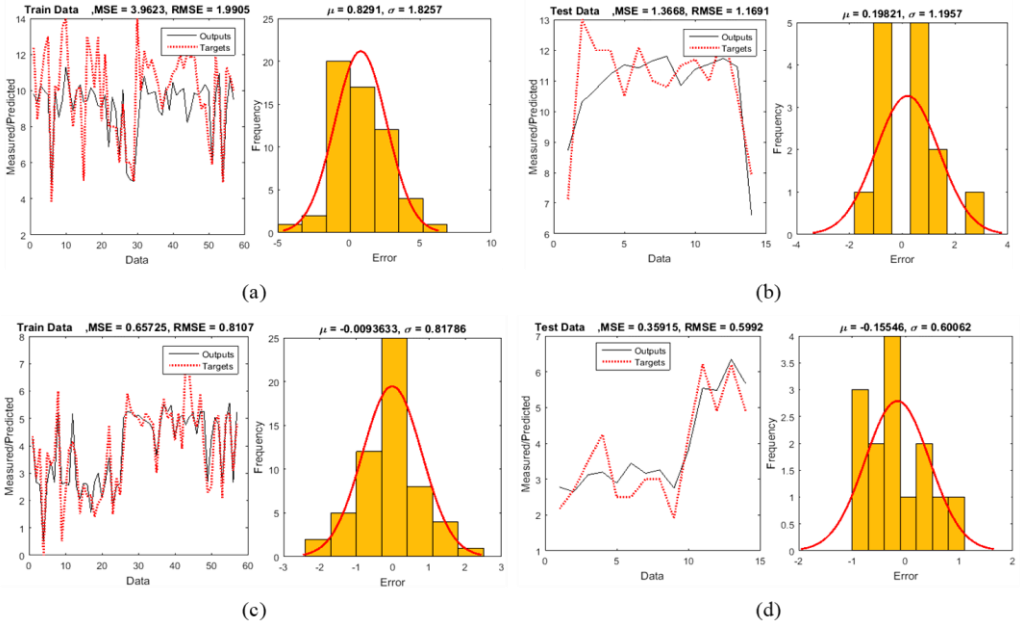

Figure 7. The measured and estimated values, and prediction error histogram for the optimum MLP. (a) training data of throw, (b) test data of throw (c) training data of drop, (d) test data of drop.

Table 4. The PCA-GA-MLP results for throw and drop.

Output	Data	NSE	RMSE	MAE	MEDAE
Throw	ALL	0.526	1.612	1.260	1.036
	Train	0.523	1.678	1.288	1.016
	Test	0.244	1.387	1.220	1.131
	validation	0.606	1.530	1.169	1.323
Drop	ALL	0.728	0.781	0.600	0.426
	Train	0.725	0.811	0.606	0.406
	Test	0.810	0.599	0.517	0.486
	validation	0.621	0.827	0.677	0.475

4. Discussion

In this section, the GA-MLP and PCA-GA-MLP models are compared. Hence, based on the indices reported in Tables 3 and 4, it is evident that integrating PCA can improve the generalization of MLP networks. However, the PCA-GA-MLP models, for both throw and drop, have lower performance in comparison. Comparing the GA-MLP and PCA-GA-MLP performances reveals that the results for the drop are better than the throw. For further comparison, the correlation between the measured and estimated values for both scenarios is shown in Figure 8. It is concluded that the results of both scenarios are acceptable except for the PCA-GA-MLP model used to predict the throw. Nevertheless, the GA-MLP models have complete superiority over the PCA-GA-MLP models.

In addition, due to the probabilistic nature of the GA, the consistency of the GA-MLP and PCA-GA-MLP models is explored by statistical analyzes. In that regard, 30 new independent runs are conducted for both scenarios, and the statistical properties for all indices (i.e., NSE, RSME, MAE, and MEDAE) are calculated. Figure 9 shows the histogram plots and normal distribution parameters for all indices. Comparing the results shows the consistency of the results. The standard deviation is shown in Figure 9, which is acceptable relative to the mean of the distributions.

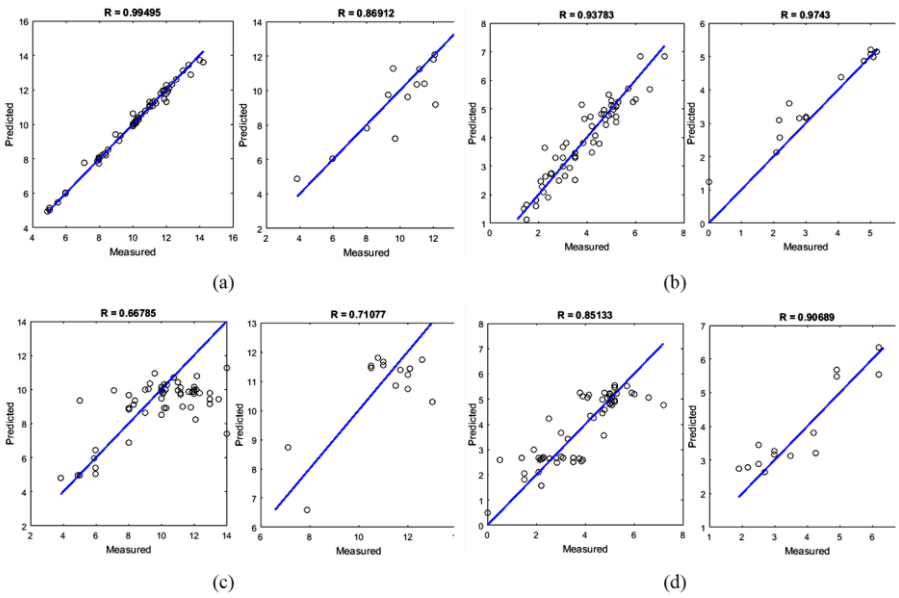

Figure 8. The correlation of the measured and estimated values. (a) the training and testing data sets for throw by the GA-MLP, (b) the training and testing data sets for drop by the GA-MLP, (c) the training and testing data sets for throw by the PCA-GA-MLP, (d) the training and testing data sets for drop by the PCA-GA-MLP.

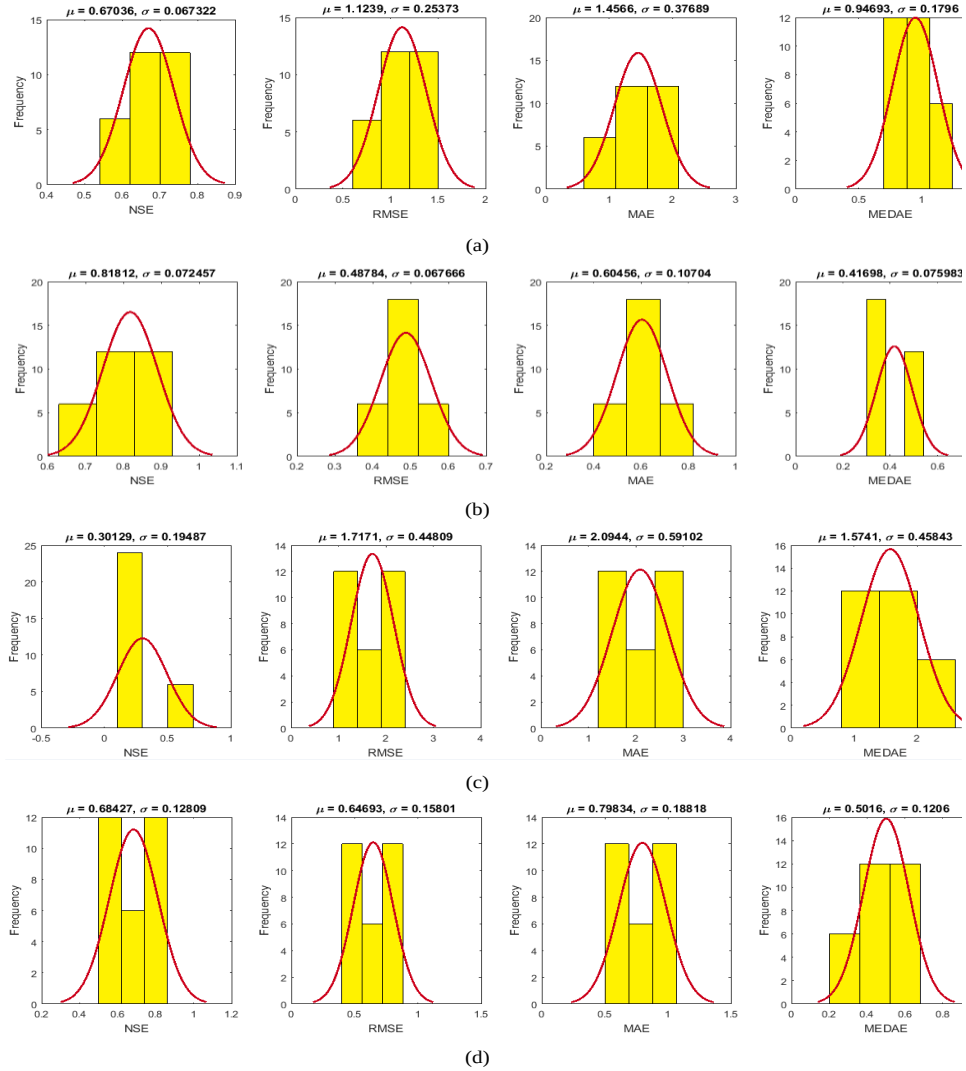

Figure 9. The model performance. (a) throw by the GA-MLP, (b) drop by the GA-MLP, (c) throw by the PCA-GA-MLP, (d) drop by the PCA-GA-MLP.

Finally, sensitivity analysis is performed for the best GA-MLP models. This study determined the significance of input variables using the "improved backward stepwise selection" approach. In this method, the sensitivity of the *MSE* is evaluated by sequentially setting input neurons to their mean values. Therefore, by using Eq. 14, the relative Importance Factor (*IF*) of each variable is determined, which is the ratio of the resulting MSE (MSE_i) to the original network *MSE* [68, 69]:

$$IF_i = \frac{MSE_i}{MSE} \quad (14)$$

The results are given in Figure 10. As in Figure 10, all the input variables significantly predict muckpile shape. However, the MLP model (Figure 4b) is more sensitive to specific charges when modeling drops. While for the throw, the MLP model (Figure 4a) is more sensitive to specific charges and sub-drilling.

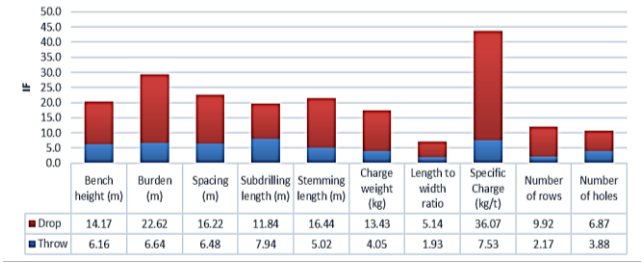

Figure 10. Sensitivity analysis and IF of input variables.

Conclusion

In open-pit mining, there is always a desired MSh. It is determined by the equipment type and size utilized and depends on the blasting blocks' features. It is essential to find an appropriate model to predict and optimize the MSh according to the blasting and rock mass parameters. Hence, a hybrid approach is used where the MLP network is prepared with the GA. Unlike the traditional trial and error procedure, the GA-MLP model is a self-organized model that finds a near-optimal architecture for an MLP with high performance and generalization. Hence, several blasting data were used to predict the MSh and validate the proposed MLP method. Principle component analysis was used for variable reduction while improving the running time of the GA-MLP. Results show that the prediction obtained by PCA-GA-MLP outperforms the others except for the throw. Comparing the results confirms the absolute superiority of the GA-ANN to the PCA-GA-MLP for both throw and drop. The best model for predicting throw has an NSE of 0.946 and 0.764 for the training and testing data sets, respectively.

Moreover, throw prediction RMSEs are 0.534 and 1.247 for the training and testing data sets, respectively. The best model for drop has NSE of 0.913 and 0.819 and RMSE of 0.455 and 0.584 for both training and testing. The sensitivity analysis shows that drop is more affected by specific charge while the throw is affected by specific charge and sub-drilling length. In future, some field tests are defined to analyze the relationship between different firing pattern and blasting performance.

REFERENCES

[1] Kose H, Aksoy CO, Gonen A, Kun M, Malli T (2005) Economic evaluation of optimum bench height in quarries. Journal of the South African Institute of Mining and Metallurgy, 105(2):127-136

[2] Afeni TB 2009 Optimization of drilling and blasting operations in an open pit mine - the SOMAIR experience. Mining Science and Technology, 19(6):736-739

[3] Azimi Y, Osanloo M, Aakbarpour-Shirazi M, Bazzazi AA (2010) Prediction of the blastability designation of rock masses using fuzzy sets. Int. J. Rock Mech. Min. Sci., 47:1126-1140, DOI: 10.1016/j.ijrmms.2010.06.016

[4] Kahriman A, Ozer U, Karadogan A, Ozdemir K, Kaya E (2008) Effects of particle size distribution on loading performance. 34th Annual Conference on Explosives and Blasting Technique, USA, January, 279-284

[5] Doktan M (2001) Impact of blast fragmentation on truck-shovel fleet performance. 17th International Mining Congress and Exhibition of Turkey, Ankara, Turkey, June, 375-379.

[6] Michaud P, Lizotte Y, Scoble M (1997) Rock fragmentation and mining productivity: characterization and case studies, 17thAnnual Conference on Explosives and Blasting Technique, USA, February, 61-72

[7] Singh PK, Roy MP, Paswan RK, Sarim M, Kumar S, Jha RR (2016) Rock fragmentation control in opencast blasting, Journal of Rock Mechanics and Geotechnical Engineering, 8(2016), 225-237

[8] Mirabedi SMM, Khodaiari A, Jafari A, Yavari M (2017) The effect of important fragmented rock properties on the penetration rate of loader bucket, Geotech Geol Eng., DOI: 10.1007/s10706-017-0393-7

[9] Tosun A (2018) A modified Wipfrag program for determining muckpile fragmentation, The journal of the Southern African Institute of Mining and Metallurgy, 118(October), 1113-1119, DOI: 10.17159/2411-9717/2018/v118n10a13

[10] Leng, Z., Fan, Y., Gao, Q., & Hu, Y. (2020). Evaluation and optimization of blasting approaches to reducing oversize boulders and toes in open-pit mine. International Journal of Mining Science and Technology, 30(3), 373-380.

[11] Tosun, A. (2022). A new method for determining muckpile fragmentation formed by blasting. Journal of the Southern African Institute of Mining and Metallurgy, 122(11), 665-672.

[12] Segarra, P., Sanchidrian, J. A., López, L. M., & Querol, E. (2010). On the prediction of mucking rates in metal ore blasting. Journal of Mining Science, 46, 167-176.

[13] Sarma S, Kanchibotla W (2010) Mine to mill process integration and optimization – benefits and challenges, 36th Annual Conference on Explosives and Blasting Technique, USA, January, 349-369

[14] Singh SP, Narendrula R (2006) Factors affecting the productivity of loaders in surface mines. International Journal of Surface Mining, Reclamation and Environment, 20(01), 20-32, DOI: 10.1016/j.jrmge.2015.10.005

[15] Aler J, Du Mouza J, Arnould M (1996) Measurement of the fragmentation efficiency of rock mass blasting and its mining applications, International Journal of Rock Mechanics and Mining Sciences & Geomechanics, 33(01), 125-139

[16] Mishra AK, Sinha M, Rout M (2013) Cast blasting for improved mine economics, in Ghose AK, Joshi A, (Eds), Blasting in mines – new trends, Taylor & Francis Group, London, ISBN 978-0-415-62139-7, 73-80

[17] Hanspal S, Scoble M, Lizotte Y (1995) Anatomy of a blast muckpile: Influence on loading machine performance. 21th Annual Conference on Explosives and Blasting Techniques, Nashville, TN, USA, February, 371p

[18] Jimeno CL, Jimeno EL, Carcedo FJA (1995) Drilling and blasting of rocks, Ramiro, Y.V.D. (translate by De Ramiro, Y.V.), A.A. Balkema, Rotterdam, Brookfield, ISBN: 90-5410-199-7, 391p

[19] Adhikari GR (2000) Empirical methods for the calculation of

the specific charge for surface blast design, Fragblast, Int. J. for Blasting and Fragmentation, 4:1, 19-33, DOI: 10.1080/13855140009408061

[20] Jhanwar, J. C., & Jethwa, J. L. (2000). The use of air decks in production blasting in an open pit coal mine. Geotechnical & Geological Engineering, 18, 269-287

[21] Silva, J., Li, L., & Gernand, J. M. (2018). Reliability analysis for mine blast performance based on delay type and firing time. *International Journal of Mining Science and Technology*, *28*(2), 195-204.

[22] Zou Z. & Jun Y. (2020). Modelling blast movement and muckpile formation with the position-based dynamics method, *International Journal of Mining, Reclamation and Environment*, DOI: 10.1080/17480930.2020.1835210

[23] Yang RL, Kavetsky A, Mckenzie CK (1989) A two-dimensional kinematic model for predicting muckpile shape in bench blasting, International Journal of Mining and Geological Engineering, 7, 209-226

[24] Yang RL, Kavetsky A (1990) A three-dimensional model of muckpile formation and grade boundary movement open pit blasting, International Journal of Mining and Geological Engineering, 8, 13-34

[25] Morin MA, Ficarazzo F (2006) Monte-Carlo simulation as a tool to predict blasting fragmentation based on the Kuz–Ram model, Computers & Geosciences, 32, 352–359

[26] Singh PK, Roy MP, Roy A, Jha SK, Singh AKB (2010) Maximizing the throw while controlling vibration within safe limits in cast blasting, Rock Fragmentation by Blasting, Sanchidrian, J.A., (ed.), Taylor & Francis Group, London

[27] Mencacci S, Jacquet D, Vandenabelle O, Chavez R, Couvrat JF, Sarrey Y (2010) Six-Sigma methodology applied to blasting, Rock Fragmentation by Blasting, Sanchidrian, J.A., (ed.), Taylor & Francis Group, London

[28] Muller B, Hausmann J, Niedzwiedz H (2010) Control of rock fragmentation and muckpile geometry during production blasts (environmentally friendly blasting technique), Rock Fragmentation by Blasting, Sanchidrian JA, (ed.), Taylor & Francis Group, London

[29] Rosa DL, Thornton D (2011) Blast movement modelling and measurement, 35th APCOM symposium, Wollongong, NSW, 24 - 30 September

[30] Choudhary BS (2013) Firing patterns and its effect on muckpile Shape parameters and fragmentation in quarry blasts, International Journal of Research in Engineering and Technology, 2(9), 32-45

[31] Choudhary BS, Rai P (2013) Stemming plug and its effect on fragmentation and muckpile shape parameters, Int. J. Mining and Mineral Engineering, 4(4), 296-311

[32] Cardu M, Seccatore J, Vaudagna A, Rezende A, Galvao F, Bettencourt J, Tomi G, (2015) Evidences of the influence of the detonation sequence in rock fragmentation by blasting, Part II, REM: R. Esc. Minas, Ouro Preto, 68(4), 455-462, DOI: 10.1590/0370-44672014680219

[33] Singh T, Singh V (2005) An intelligent approach to prediction and control ground vibration in mines, Geotech Geol Eng, 23, 249-262

[34] Sharma, A., Mishra, A. K., & Choudhary, B. S. (2019). Impact of blast design parameters on blasted muckpile profile in building stone quarries. In Annales de Chimie Science des Materiaux, 43(1), 29-36

[35] Choudhary, B. S., & Arora, R. (2018). Influence of front row burden on fragmentation, muckpile shape, excavator cycle time, and back break in surface limestone mines. Iranian Journal of Earth Sciences, 10(1), 1-10.

[36] Choudhary, B. S. (2019). Effect of blast induced rock fragmentation and muckpile angle on excavator performance in surface mines. Mining of Mineral Deposits, 13(3), 119-126

[37] Rai P, Chatterjee S, Bandopadhyay S (2009) Neural network based selection of design parameters governing shape and powder factor of blasted muck piles: a case study, Mining Technology, 118(2), 67-78

[38] Raina AK Murthy VMSR (2016) Importance and sensitivity of variables defining throw and flyrock in surface blasting by artificial neural network method, Current Science, 111(9), 1524-1531

[39] Murthy VMSR, Kumar A, Sinha PK (2016) Prediction of throw in bench blasting using neural networks: an approach, Neural Computing and Applications, 29(1), 143-156, DOI: 10.1007/s00521-016-2423-4

[40] Vasylchuk YV, Deutsch CV (2017) Improved grade control in open pit mines, Mining Technology, DOI: 10.1080/14749009.2017.1363991

[41] Singh SP, VanDoorselaere D (2015) The relationship between blasting parameters and muckpile configuration, in Proceedings 11th International Symposium on Rock Fragmentation by Blasting, 369–374 (AusIMM)

[42] Singh SP, Cheung D (2017) Factors governing the muckpile Characteristics, International Society of Explosives Engineers, 43rd annual conference on explosives and blasting techniques, At Orlando, Florida, USA

[43] Gandomi AH, Alavi AH, Mousavi M, Tabatabaei SM (2011) A hybrid computational approach to derive new ground-motion prediction equations, Engineering Applications of Artificial Intelligence, 24(4), 717-732, DOI: 10.1016/j.engappai.2011.01.005

[44] Amiri M, Amnieh HB, Hasanipanah M, Khanli LM (2016) A new combination of artificial neural network and K-nearest neighbors' models to predict blast-induced ground vibration and air-overpressure, Eng Comput, 32, 631-644.

[45] Azimi Y, Khoshrou SH, Osanloo M (2019) Prediction of blast induced ground vibration (BIGV) of quarry mining using hybrid genetic algorithm optimized artificial neural network, Measurement, 147, 106874, DOI: 10.1016/j.measurement.2019.106874.

[46] Gao W, Alqahtani AS, Mubarakali A, Mavaluru D, Khalafi S (2020) Developing an innovative soft computing scheme for prediction of air overpressure resulting from mine blasting using GMDH optimized by GA. Engineering with Computers 36, 647–654, DOI: 10.1007/s00366-019-00720-5

[47] Zhang S, Bui XN, Trung NT, Nguyen H, Bui H (2020) Prediction of rock size distribution in mine bench blasting using a novel ant colony optimization-based boosted regression tree technique, Nat Resour Res, 29, 867–886, DOI: 10.1007/s11053-019-09603-4

[48] Ke B, Nguyen H, Bui XN, Costache R (2021) Estimation of ground vibration intensity induced by mine blasting using a state-of-the-art hybrid autoencoder neural network and support vector regression model, Nat Resour Res, DOI: 10.1007/s11053-021-09890-w

[49] Castillo PA, Merelo JJ, González J, Rivas V, Romero G (1999) SA-Prop: Optimization of multilayer perceptron parameters

using simulated annealing, International Work-Conference on Artificial Neural Networks, Springer, 661-670.

[50] Socha K, Blum C (2007) An ant colony optimization algorithm for continuous optimization: application to feed-forward neural network training, Neural Computing and Applications, 16, 235-247.

[51] Moghaddam MA, Golmezergi R, Kolahan F (2016) Multi-variable measurements and optimization of GMAW parameters for API-X42 steel alloy using a hybrid BPNN–PSO approach, Measurement, 92, 279-287.

[52] Campos LML, Oliveira RCL, Roisenberg M (2016) Optimization of neural networks through grammatical evolution and a genetic algorithm, Expert Syst. Appl., 56, 368-384.

[53] Ekonomou L (2010) Greek long-term energy consumption prediction using artificial neural networks, Energy, 35, 512-517.

[54] Azimi Y (2019) Prediction of seismic wave intensity generated by bench blasting using intelligence committee machines. International Journal of Engineering, 32(4), 617-627.

[55] Goldberg D (1989) Genetic Algorithms in Search, Optimization, and Machine Learning, Addison Wesley, Reading, Massachusetts

[56] Carvalho AR, Ramos FM, Chaves AA (2011) Metaheuristics for the feedforward artificial neural network (ANN) architecture optimization problem, Neural Computing and Applications, 20, 1273-1284.

[57] Deb K (2000) An efficient constraint handling method for genetic algorithms. Computer methods in applied mechanics and engineering, 186(2-4), 311-338.

[58] Deep K, Singh KP, Kansal ML, Mohan C (2009) A real coded genetic algorithm for solving integer and mixed integer optimization problems. Applied Mathematics and Computation, 212(2), 505-518.

[59] Cunningham P, Carney J, Jacob S (2000) Stability problems with artificial neural networks and the ensemble solution, Artif Intell Med, 20(3), 217–25, DOI: 10.1016/S0933-3657(00)00065-8

[60] Chan ZSH, Ngan HW, Rad AB, David AK, Kasabov N (2006) Short-term ANN load forecasting from limited data using generalization learning strategies, Neurocomputing, 70, 409–419, DOI: 10.1016/j.neucom.2005.12.131

[61] Shao Y, Lunetta RS (2012) Comparison of support vector machine, neural network, and CART algorithms for the land-cover classification using limited training data points, ISPRS Journal of Photogrammetry and Remote Sensing 70, 78–87, DOI: 10.1016/j.isprsjprs.2012.04.001

[62] Li D, Chen H, Shi Q (2018) Learning from small datasets containing nominal attributes, Neurocomputing, 291, 226–236, DOI: 10.1016/j.neucom.2018.02.069

[63] Koziarski M, Krawczyk B, Wozniak M (2019) Radial-based oversampling for noisy imbalanced data classification, Neurocomputing, 343, 19–33, DOI: 10.1016/j.neucom .2018.04.089

[64] Espezua S, Villanueva E, Maciel CD, Carvalho A (2015) A Projection Pursuit framework for supervised dimension reduction of high dimensional small sample datasets, Neurocomputing, 149, 767–776, DOI: 10.1016/j.neucom. 2014.07.057

[65] Yang X, Huang K, Zhang R, Goulermas JY, Hussain A (2018) A new two-layer mixture of factor analyzers with joint factor loading model for the classification of small dataset problems, Neurocomputing, 312, 352–363, DOI: 10.1016/j.neucom. 2018.05.085

[66] Ojha VK, Abraham A, Snasel V (2017) Metaheuristic design of feedforward neural networks: A review of two decades of research, Engineering Applications of Artificial Intelligence, 60, 97-116, DOI: 10.1016/j.engappai.2017.01.013

[67] Jackson JE (1991) A user's guide to principal components. John Wiley & Sons, New York, USA, 592 p

[68] Gevrey M, Dimopoulos I, Lek S (2003) Review and comparison of methods to study the contribution of variables in artificial neural network models, Ecological modelling 160(3), 249-264, DOI: 10.1016/S0304-3800(02)00257-0

[69] Olden JD, Joy MK, Death RG (2004) An accurate comparison of methods for quantifying variable importance in artificial neural networks using simulated data." Ecological modelling 178(3-4), 389-397, DOI: 10.1016/j.ecolmodel.2004.03.013